Z. Phys. C – Particles and Fields 53, 73–77 (1992)

Zeitschrift für Physik C Particles and Fields

Precision measurement of structure function ratios for ^{6}Li, ^{12}C and ^{40}Ca

New Muon Collaboration (NMC)

P. Amaudruz[12,a], M. Arneodo[13], A. Arvidson[14], B. Badelek[16], G. Baum[1], J. Beaufays[9,b], I.G. Bird[4,c], M. Botje[12], C. Broggini[8,d], W. Brückner[4], A. Brüll[3], W.J. Burger[12,e], J. Ciborowski[9,f], R. van Dantzig[9], H. Döbbeling[4,g], J. Domingo[12,h], J. Drinkard[11], H. Engelien[3], M.I. Ferrero[13], L. Fluri[8], P. Grafstrom[14,i], D. von Harrach[4,j], M. van der Heijden[9], C. Heusch[11], Q. Ingram[12], K. Janson[14], M. de Jong[9], E.M. Kabuß[4,j], R. Kaiser[3], T.J. Ketel[9], F. Klein[6], B. Korzen[17], U. Krüner[17], S. Kullander[14], U. Landgraf[3], F. Lettenström[11], T. Lindqvist[14], G.K. Mallot[6], C. Mariotti[13], G. van Middelkoop[2,9], Y. Mizuno[4,k], J. Nassalski[15,9], D. Nowotny[4], N. Pavel[17,l], C. Peroni[13], H. Peschel[17,m], B. Povh[4,5], R. Rieger[6], K. Rith[4], K. Röhrich[6,n], E. Rondio[16], L. Ropelewski[16], A. Sandacz[15], C. Scholz[4], R. Schumacher[12,o], U. Sennhauser[12,p], F. Sever[1,q], T.-A. Shibata[5], M. Siebler[1], A. Simon[4], A. Staiano[13], G. Taylor[10,r], M. Treichel[4,s], J.L. Vuilleumier[8], T. Walcher[6], R. Windmolders[7], F. Zetsche[4]

[1] Bielefeld University, W-4800 Bielefeld, Federal Republic of Germany[t]
[2] CERN, CH-1211 Geneva 23, Switzerland
[3] Freiburg University, W-7800 Freiburg, Federal Republic of Germany[t]
[4] MPI Heidelberg, W-6900 Heidelberg, Federal Republic of Germany[t]
[5] Heidelberg University, W-6900 Heidelberg, Federal Republic of Germany[t]
[6] Mainz University, W-6500 Mainz, Federal Republic of Germany[t]
[7] Mons University, B-7000 Mons, Belgium
[8] Neuchâtel University, CH-2000 Neuchâtel, Switzerland
[9] NIKHEF-K, NL-1009 AJ Amsterdam, The Netherlands[u]
[10] Oxford University, Oxford OX1 3RH, UK
[11] University of California, Santa Cruz, CA 95064, USA
[12] Paul Scherrer Institute, CH-5234 Villingen, Switzerland
[13] Torino University and INFN, I-10125 Torino, Italy
[14] Uppsala University, S-75121 Uppsala, Sweden
[15] Institute for Nuclear Studies, PL-00-681 Warsaw, Poland[v]
[16] Warsaw University, PL-00-681 Warsaw, Poland[w]
[17] Wuppertal University, W-5600 Wuppertal, Federal Republic of Germany[t]

Received 2 September 1991

Abstract. The structure function ratios $F_2^{\mathrm{C}}/F_2^{\mathrm{Li}}$, $F_2^{\mathrm{Ca}}/F_2^{\mathrm{Li}}$ and $F_2^{\mathrm{Ca}}/F_2^{\mathrm{C}}$ were measured in deep inelastic muon-nucleus scattering at an incident muon energy of 90 GeV, covering the kinematic range $0.0085<x<0.6$ and $0.8<Q^2<17\,\mathrm{GeV}^2$. The sensitivity of the nuclear structure functions to the size and mean density of the target nucleus is discussed.

The structure functions per nucleon, F_2, for deep inelastic scattering of muons or electrons on deuterium and on heavier nuclei are not the same (EMC effect). This effect has been observed in a number of experiments [1–9] covering the range of values of the Bjorken scaling variable x between 0.002 and 0.8.

In the one photon exchange approximation and

---

[a] Now at TRIUMF, Vancouver, BC, Canada
[b] Now at Trasys, Brussels, Belgium
[c] Now at NIKHEF-K, P.O. Box 4395, 1009 AJ Amsterdam, The Netherlands
[d] Now at INFN, Laboratori Nazionali del Gran Sasso, 67010 Assergi, Italy
[e] Now at Université de Genève, 1211 Genève 4, Switzerland
[f] Now at University of Warsaw, 00681 Warsaw, Poland
[g] Now at GSI, 6100 Darmstadt, FRG
[h] Now at CEBAF, Newport News, VA, USA
[i] Now at CERN, 1211 Geneva 23, Switzerland
[j] Now at University of Mainz, 6500 Mainz, FRG
[k] Now at Osaka University, Osaka, Japan
[l] Now at DESY, Hamburg, FRG
[m] Now at Gruner and Jahr AG & CoKG, Itzehoe, FRG
[n] Now at IKP2-KFA, Jülich, FRG
[o] Now at Carnegie Mellon University, Pittsburgh, USA
[p] Now at EMPA, 8600 Dübendorf, Switzerland
[q] On leave from Jozef Stefan Institut, Ljubljana, Yugoslavia, now at DPhN Saclay, 91191 Gif-sur-Yvette, France
[r] Now at University of Melbourne, Parkville, Victoria, Australia
[s] Now at Université de Neuchâtel, Switzerland
[t] Supported by Bundesministerium für Forschung und Technologie
[u] Supported in part by FOM, Vrije Universiteit Amsterdam and NWO
[v] Supported by CPBP.01.06
[w] Supported by CPBP.01.09

neglecting the muon mass, the deep inelastic differential cross section per nucleon on a nucleus A can be written as

$$\frac{d^2\sigma^A(x,Q^2)}{dx\,dQ^2}=\frac{4\pi\alpha^2}{Q^4x}F_2^A(x,Q^2)\cdot\left\{1-y-\frac{Q^2}{4E^2}+\frac{y^2+Q^2/E^2}{2[1+R^A(x,Q^2)]}\right\},\qquad(1)$$

where $x=Q^2/2M\nu$ and $y=\nu/E$ are the usual scaling variables and where $-Q^2$ is the squared four momentum transfer, E the energy of the incident muon in the laboratory, ν the energy of the virtual photon in the laboratory and M the proton mass. In (1), $F_2^A(x,Q^2)$ is the nuclear structure function per nucleon and $R^A(x,Q^2)$ is the ratio of total absorption cross sections for longitudinally and transversely polarised virtual photons on a nucleus A. Assuming that R^A is independent of A, which is consistent with the experimental data for $x>0.2$ and $Q^2>1$ GeV^2 [10], the ratio $F_2^{A_1}/F_2^{A_2}$ is equal to the corresponding cross section ratio.

The x dependence of the structure function ratio F_2^A/F_2^D for a nucleus A relative to deuterium is characterised by: (i) a depletion below unity at small x; (ii) a maximum above unity at intermediate $x\approx0.1$–0.2; (iii) a minimum below unity at $x\approx0.7$ and (iv) a sharp rise at larger x. The structure function ratio at small and intermediate x is usually described in terms of generalised vector meson dominance or partonic models [11]. In both descriptions the nuclear size and the mean nuclear density are relevant parameters.

In a recent publication [12] we reported on the x and Q^2 dependence of the structure function ratios F_2^A/F_2^D for ^{4}He, ^{12}C and ^{40}Ca, measured at 200 GeV incident muon energy. In the present experiment at 90 GeV, the ratios $F_2^{A_1}/F_2^{A_2}$ were studied for the nuclei ^{6}Li, ^{12}C and ^{40}Ca as a function of x. This provides a comparison, in one experiment, of structure functions for pairs of isoscalar nuclei differing primarily either in radius (r) or density (ρ). In particular ^{6}Li ($r=2.6$ fm, $\rho=0.04$ fm^{-3}) and ^{12}C ($r=2.5$ fm, $\rho=0.09$ fm^{-3}) have equal radii but different densities, whereas ^{12}C and ^{40}Ca ($r=3.5$ fm, $\rho=0.11$ fm^{-3}) differ more in radius than in density [13].

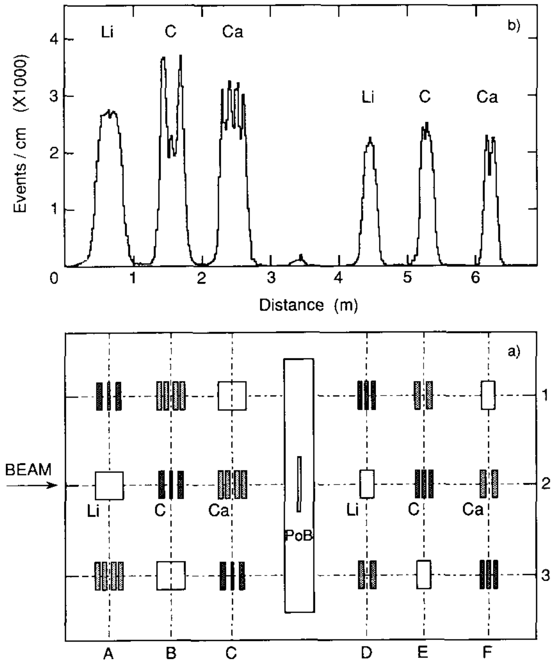

Fig. 1. **a** Platform with the multiple target setup. Targets aligned longitudinally in rows (1–3) are exposed to the same beam flux, those aligned transversely ($A-F$) have the same spectrometer acceptance; P0B is a small wire chamber. **b** Distribution of reconstructed interaction vertices for the middle row of targets

The measurements were performed at the CERN SPS muon beam line (M2) using the NMC spectrometer [14, 15], an upgrade of that of the European Muon Collaboration (EMC) [16, 8]. A novel feature was the multiple target arrangement. Targets of the different materials were placed in a row at longitudinally well separated locations along the spectrometer axis and exposed simultaneously to the beam. Three such rows, differing in the ordering of materials, were placed on a common platform (Fig. 1a). The calcium and carbon targets were segmented and distributed over a length equal to that of the lower density lithium targets. The rows of targets were positioned in the beam in turn by lateral displacement of the platform at approximately 30 min intervals. In each row the targets were arranged in an upstream and a downstream group, within which the targets had approximately the same thickness, 20 g/cm^2 (upstream) and 10 g/cm^2 (downstream). Figure 1b shows, for one row of targets, the longitudinal distribution of reconstructed interaction vertices. It is seen in this figure that the different targets were well resolved.

With this target arrangement beam flux and spectrometer acceptance corrections cancel in the calculation of the cross section ratio $\sigma^{A_1}/\sigma^{A_2}$ for the nuclei A_1 and A_2. This ratio thus depends only on the radiatively corrected numbers of events $N_i^{A_1(A_2)}$ and on the numbers of nucleons per unit area $T_i^{A_1(A_2)}$:

$$\frac{\sigma^{A_1}}{\sigma^{A_2}}=\left[\prod_{i=1}^{3}\frac{N_i^{A_1}}{N_i^{A_2}}\frac{T_i^{A_2}}{T_i^{A_1}}\right]^{\frac{1}{3}},\qquad(2)$$

where i indicates the target row. These ratios were evaluated for the upstream and downstream target groups separately. The final values are the geometrical mean of the ratios for the two groups, weighted by their statistical errors. A more detailed description of the experimental method can be found in [15].

To obtain the one photon exchange cross section (1) the measured event yields were corrected for radiative effects. A radiative correction weight factor was attributed to each event depending on the scaling variables x, y and on the target material. This weight was calculated as in previous analyses [9, 12] using the procedure of Mo and Tsai [17]. The resulting mean corrections to the cross section ratios were largest for the lowest x bin where they amounted to 7% (C/Li), 23% (Ca/Li) and 18% (Ca/C). For $x > 0.05$ they were smaller than 1%.

A correction for the effects of the finite kinematic resolution was obtained from a Monte Carlo simulation of the experiment. Corrections made for attribution of events to the wrong target were calculated from the tails in the distributions of the reconstructed interaction vertices (see Fig. 1b). Contributions from corrosion layers on the lithium and calcium targets and from their protection foils were also corrected for. None of these corrections was significant for $x > 0.04$ and for the lowest x bin they were at most 0.5%. Corrections for the isotopic impurities of the targets and the air between the targets were negligible.

The final data sample consisted of 1.4 million events, after having rejected events with $x < 0.007$, muon scattering angle $\theta < 12$ mrad for the upstream target group and $\theta < 14$ mrad for the downstream group, scattered muon energy $E' < 10$ GeV and $\nu < 10$ GeV. A cut depending on x and y was applied to keep the radiative correction weight factor for each event larger than 0.5. The measured ratios at small x are in good agreement with those obtained from a subset of the data where the observation of at least one energetic hadron was required in each event [18]. Such a requirement removes the coherent nuclear radiative events which cause the major part of the correction.

The main sources of systematic uncertainties in the measurements are the following:

(1) The input to the radiative correction procedure (parametrisation of the nuclear structure functions F_2^A and R^A and of the nuclear form factors). The resulting uncertainty is at most 2.7%, for Ca/Li at $x = 0.0085$, and decreases to 0.1% for $x > 0.05$.

(2) The assignment of events to the wrong target, which contributed less than 0.2% uncertainty.

(3) Averaging over Q^2 within each x bin, which gave an estimated uncertainty of up to 0.2%.

The total systematic errors were obtained by adding these contributions in quadrature. Overall normalisation errors of 0.7% (C/Li), 0.8% (Ca/Li) and 0.5% (Ca/C) are due to uncertainties in the target thicknesses.

The measured ratios are presented in Table 1 and in Figs. 2 and 3. The Ca/C ratio derived from earlier NMC data for C/D and Ca/D [12] at 200 GeV is also shown in Fig. 3. These data, measured at larger values of Q^2, are in agreement with the present results. This is consistent with our previous conclusion [12] that the C/D and Ca/D ratios do not depend significantly on Q^2. The following observations can be made from the data.

(i) At small x there is a depletion of the structure function in C relative to that in Li, which has the same radius but a lower mean density. However, the structure function depletion in Ca relative to that in Li is twice as large, implying that the depletion increases with both radius and density.

Table 1. Values of structure function ratios $F_2^{A_1}/F_2^{A_2}$, averaged over Q^2 (normalisation uncertainties are not included in the errors)

x	$\langle Q^2 \rangle$ [GeV^2]	F_2^{C}/F_2^{Li}	stat.	syst.
0.00850	0.84	0.905	0.009	0.012
0.01125	1.1	0.951	0.010	0.009
0.01375	1.2	0.963	0.010	0.007
0.01625	1.4	0.952	0.010	0.005
0.01875	1.6	0.987	0.011	0.004
0.0225	1.8	0.971	0.008	0.004
0.0275	2.0	0.964	0.008	0.003
0.0325	2.2	0.974	0.009	0.002
0.0375	2.3	0.979	0.009	0.002
0.0425	2.4	1.001	0.010	0.002
0.0475	2.6	0.998	0.010	0.002
0.0525	2.7	1.019	0.011	0.002
0.0575	2.8	1.020	0.012	0.002
0.0650	3.0	0.999	0.009	0.002
0.0750	3.3	1.012	0.009	0.002
0.0850	3.6	1.004	0.010	0.002
0.0950	3.9	1.009	0.011	0.002
0.1125	4.3	1.028	0.008	0.002
0.1375	5.1	1.012	0.010	0.002
0.175	6.2	1.019	0.009	0.002
0.225	7.7	1.003	0.013	0.002
0.275	9.1	1.001	0.017	0.002
0.35	11	0.989	0.017	0.002
0.45	14	0.967	0.028	0.002
0.60	17	1.015	0.040	0.004

x	$\langle Q^2 \rangle$ [GeV^2]	F_2^{Ca}/F_2^{Li}	stat.	syst.
0.00850	0.84	0.838	0.008	0.022
0.01125	1.1	0.868	0.009	0.017
0.01375	1.2	0.900	0.009	0.013
0.01625	1.4	0.906	0.010	0.010
0.01875	1.6	0.958	0.010	0.008
0.0225	1.8	0.935	0.007	0.006
0.0275	2.0	0.935	0.008	0.004
0.0325	2.2	0.964	0.009	0.003
0.0375	2.3	0.980	0.009	0.002
0.0425	2.4	0.974	0.010	0.002
0.0475	2.6	0.965	0.010	0.002
0.0525	2.7	1.010	0.011	0.002
0.0575	2.8	1.011	0.011	0.002
0.0650	3.0	1.005	0.008	0.002
0.0750	3.3	1.007	0.009	0.002
0.0850	3.6	1.012	0.010	0.002
0.0950	3.9	1.010	0.011	0.002
0.1125	4.3	1.020	0.008	0.002
0.1375	5.1	1.017	0.010	0.002
0.175	6.2	1.018	0.009	0.002
0.225	7.7	1.017	0.013	0.002
0.275	9.1	0.998	0.016	0.002
0.35	11	0.984	0.017	0.002
0.45	14	0.990	0.028	0.002
0.60	17	0.969	0.038	0.004

x	$\langle Q^2 \rangle$ [GeV^2]	F_2^{Ca}/F_2^{C}	stat.	syst.
0.00850	0.84	0.926	0.009	0.023
0.01125	1.1	0.913	0.009	0.015
0.01375	1.2	0.934	0.010	0.011
0.01625	1.4	0.952	0.010	0.008
0.01875	1.6	0.970	0.010	0.007
0.0225	1.8	0.962	0.008	0.005
0.0275	2.0	0.970	0.008	0.003
0.0325	2.2	0.989	0.009	0.003

Table 1 (continued)

x	$\langle Q^2\rangle$ [GeV^2]	$F_2^{\mathrm{Ca}}/F_2^{\mathrm{C}}$	stat.	syst.
0.0375	2.3	1.001	0.009	0.002
0.0425	2.4	0.973	0.009	0.002
0.0475	2.6	0.968	0.010	0.002
0.0525	2.7	0.991	0.010	0.002
0.0575	2.8	0.991	0.011	0.002
0.0650	3.0	1.006	0.008	0.002
0.0750	3.3	0.994	0.009	0.002
0.0850	3.6	1.008	0.010	0.002
0.0950	3.9	1.001	0.011	0.002
0.1125	4.3	0.993	0.008	0.002
0.1375	5.1	1.006	0.010	0.002
0.175	6.2	1.000	0.009	0.002
0.225	7.7	1.014	0.012	0.002
0.275	9.1	0.997	0.016	0.002
0.35	11	0.995	0.017	0.002
0.45	14	1.024	0.029	0.002
0.60	17	0.955	0.036	0.002

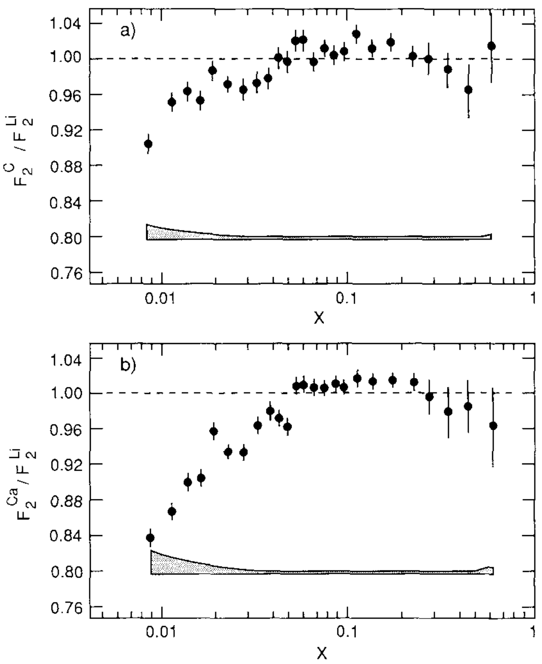

Fig. 2a, b. The measured structure function ratios as functions of x, averaged over Q^2 **a** for carbon and lithium (C/Li); **b** for calcium and lithium (Ca/Li). The bars represent the statistical errors. The systematic uncertainties are indicated by bands; the normalisation uncertainties (not included in the errors) are 0.7% and 0.8% for C/Li and Ca/Li, respectively

(ii) At intermediate x, the structure functions in the nuclei with high density, C and Ca, exhibit similar enhancements of 1–2% relative to that in Li. There are no significant differences between the C and Ca structure functions for x between 0.07 and 0.4. This indicates a weak dependence of the structure function on the density with little or no sensitivity to the radius in the intermediate x region.

Combining the current results with those of the earlier 200 GeV measurements [12], we obtained the Li/D ratio, where it has been assumed that there is no Q^2 dependence. This ratio is compared to that of He/D [12] in Fig. 4. These two ratios are remarkably similar and indeed if one makes a bin to bin comparison, the Li/He ratio is consistent with unity over the common x range. For small x this observation is in agreement with the dependence on radius and density in (i) above: Li as compared to He ($r = 1.7$ fm, $\rho = 0.09\ \mathrm{fm}^{-3}$) has a much larger radius and a much smaller density, so that in this region two opposing dependences should tend to cancel. In the intermediate x region the weakness of the radius and density dependence, precludes, in view of the experimental uncertainties, a useful comparison with the observation (ii) above.

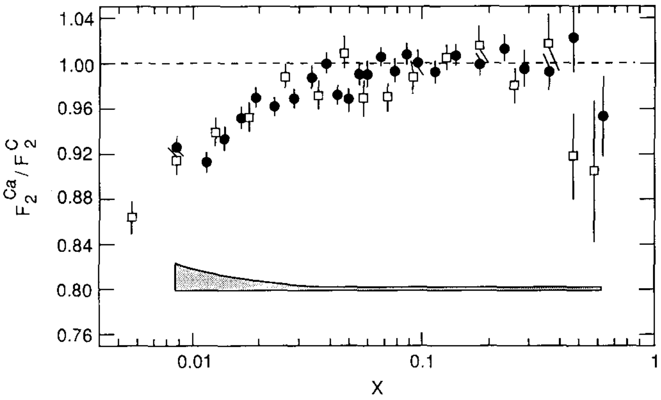

Fig. 3. Same as Fig. 2 for Ca/C (full symbols). The normalisation uncertainty (not included in the errors) is 0.5%. The results obtained by dividing the Ca/D and C/D ratios from the recent NMC measurement at 200 GeV [12] are indicated by squares (statistical errors only)

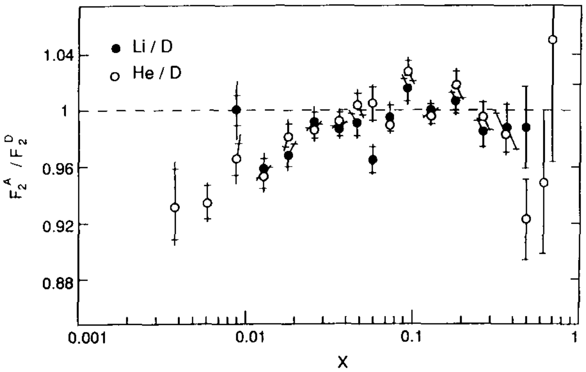

Fig. 4. The ratio for Li/D, obtained from combining the current results with the earlier measurements on C/D and Ca/D [12] at 200 GeV, compared to that for He/D [12] at 200 GeV. The inner error bars represent the statistical errors, the outer ones the statistical and systematic errors added in quadrature. Normalisation uncertainties (0.7% for Li/D and 0.4% for He/D) are not shown

In conclusion, the present data indicate a sensitivity of the EMC effect to the nuclear radius and to the mean nuclear density. At intermediate x the weak enhancement shows only a small sensitivity to the nuclear density while at small x the strong depletion appears to depend on both radius and density.

References

1. SLAC-E61, S. Stein et al.: Phys. Rev. D12 (1975) 1884
2. FNAL, M.S. Goodman et al.: Phys. Rev. Lett. 47 (1981) 293
3. SLAC-E87, E49b, A. Bodek et al.: Phys. Rev. Lett. 50 (1983) 1431; ibid. 51 (1983) 534
4. CERN-NA2/EMC, J.J. Aubert et al.: Phys. Lett. B123 (1983) 275
5. SLAC-E139, R.G. Arnold et al.: Phys. Rev. Lett. 52 (1984) 727; R.G. Arnold et al.: SLAC-PUB-3257 (1983)
6. CERN-NA4/BCDMS, G. Bari et al.: Phys. Lett. B163 (1985) 282
7. CERN-NA4/BCDMS, A.C. Benvenuti et al.: Phys. Lett. B189 (1987) 483
8. CERN-NA2'/EMC, J. Ashman et al.: Phys. Lett. B202 (1988) 603
9. CERN-NA28/EMC, M. Arneodo et al.: Phys. Lett. B211 (1988) 493; M. Arneodo et al.: Nucl. Phys. B333 (1990) 1
10. SLAC-E140, S. Dasu et al.: Phys. Rev. Lett. 60 (1988) 2591
11. L. Frankfurt, M. Strikman: Phys. Rep. 160 (1988) 235; R.J.M. Covolan, E. Predazzi, in: "Problems of fundamental modern physics", R. Cherubini, P. Dalpiaz, B. Minetti (eds.), p. 85; Singapore: World Scientific, 1991; L.L. Frankfurt, M.I. Strikman, in: "Electromagnetic interactions with nuclei", B. Frois, I. Sick (eds.). Singapore: World Scientific, 1991
12. CERN-NA37/NMC, P. Amaudruz et al.: Z. Phys. C – Particles and Fields 51 (1991) 387
13. Densities ρ were obtained using the formula: $\rho(A) = A/[\frac{4}{3}\pi(\frac{5}{3}\langle r^2\rangle)^{\frac{3}{2}}]$, where $\langle r^2\rangle$ is the mean square nuclear charge radius given in H. de Vries et al.: Atomic Data and Nuclear Data Tables 36 (1987) 495
14. CERN-NA37/NMC, D. Allasia et al.: Phys. Lett. B249 (1990) 366
15. CERN-NA37/NMC, P. Amaudruz et al.: CERN-PPE/91–167 (1991), to appear in Nucl. Phys. B
16. CERN-NA2/EMC, O.C. Allkofer et al.: Nucl. Instrum. Methods 179 (1981) 445
17. L.W. Mo, Y.S. Tsai: Rev. Mod. Phys. 41 (1969) 205; Y.S. Tsai: SLAC-PUB-848 (1971)
18. C. Broggini: Ph. D. thesis, University of Neuchâtel (1989); for the method see also A. Staiano: Ph. D. thesis, University of Heidelberg (1989)